Completion of cytokinesis in *C. elegans* requires a brefeldin A-sensitive membrane accumulation at the cleavage furrow apex

Ahna R. Skop*§, Dominique Bergmann†¶, William A. Mohler*¥ and John G. White*‡

Background: The terminal phase of cytokinesis in eukaryotic cells involves breakage of the intercellular canal containing the spindle midzone and resealing of the daughter cells. Recent observations suggest that the spindle midzone is required for this process. In this study, we investigated the possibility that targeted secretion in the vicinity of the spindle midzone is required for the execution of the terminal phase of cytokinesis.

Results: We inhibited secretion in early *C. elegans* embryos by treatment with brefeldin A (BFA). Using 4D recordings of dividing cells, we showed that BFA induced stereotyped failures in the terminal phase of cytokinesis; although the furrow ingressed normally, after a few minutes the furrow completely regressed, even though spindle midzone and midbody microtubules appeared normal. In addition, using an FM1-43 membrane probe, we found that membrane accumulated locally at the apices of the late cleavage furrows that form the persisting intercellular canals between daughter cells. However, in BFA-treated embryos this membrane accumulation did not occur, which possibly accounts for the observed cleavage failures.

Conclusions: We have shown that BFA disrupts the terminal phase of cytokinesis in the embryonic blastomeres of *C. elegans*. We observed that membrane accumulates at the apices of the late cleavage furrow by means of a BFA-sensitive mechanism. We suggest that this local membrane accumulation is necessary for the completion of cytokinesis and speculate that the spindle midzone region of animal cells is functionally equivalent to the phragmoplast of plants and acts to target secretion to the equatorial plane of a cleaving cell.

Addresses: *Laboratory of Molecular Biology and †Department of Molecular, Cellular, and Developmental Biology, University of Colorado, Boulder, Colorado 80309, USA. ‡Department of Anatomy, University of Wisconsin-Madison, Madison, Wisconsin 53706, USA.

Current Addresses: §Department of Molecular and Cell Biology, University of California-Berkeley, Berkeley, California 94720, USA. ¶Department of Plant Biology, Carnegie Institution of Washington and Department of Biological Sciences, Stanford University, Stanford, California 94305, USA. ¥Department of Developmental Biology, University of Connecticut Health Center, Farmington, Connecticut 06030, USA.

Correspondence: John G. White
E-mail: jwhite1@facstaff.wisc.edu

Introduction

Cytokinesis takes on a variety of manifestations in different organisms, although there are two main strategies for cleaving a cell: that used in animal cells and that used in plant cells. When a plant cell divides, a septum is formed by the migration of Golgi-derived vesicles along the microtubules of the phragmoplast toward the equatorial plane, where they fuse and form the cell plate [1]. In contrast, when an animal cell divides, an equatorial, actomyosin contractile ring assembles midway between the poles of the mitotic spindle and constricts to form the cleavage furrow [2]. At telophase, the ingressing furrow meets the midzone of the disassembling mitotic spindle. This structure persists for some time and forms a narrow intercellular bridge [3]. The intercellular bridge must be broken and the membrane must reseal in order for the daughter cells to completely separate [4].

Recent observations suggest that the final phase of cytokinesis in animal cells requires intact spindle midzone mi-crotubules [5–9] and possibly centrosomes [10]. Microtubules have been shown to be required for furrow progression and membrane insertion in the region of an advancing cleavage furrow in cleaving *Xenopus* embryos [11, 12]. Recent observations of *Drosophila* neuroblasts have shown that midbody microtubules move basally toward the cleavage site only after the cell membrane has invaginated [13], and these observations suggest that the microtubules may be necessary during post-furrow invagination steps. Although microtubules have been shown to be essential for the completion of cytokinesis [11], is it not known what additional mechanisms are required to finally separate daughter cells from one another.

A number of studies have shown that secretion is involved in the formation of the cell plate between dividing plant cells. In tobacco cells, the fungal metabolite brefeldin A has been shown to inhibit cytokinesis [14]. Mutants in the KNOLLE gene of *Arabidopsis* have defects in cytokinesis [15] and appear to be specifically defective in the fusion

of vesicles with the forming cell plate [16]. The KNOLLE gene has strong similarities to animal syntaxins, a class of proteins that is required for vesicle fusion [15]. Interestingly, syntaxin I has been shown to be required for cellularization in *Drosophila* embryos, and this finding suggests that secretion has a role in the formation of membranes around the syncytial nuclei during cellularization, a process that has similarities to cytokinesis [17]. Syntaxins are also necessary during furrow invagination in sea urchins and in *C. elegans* [18, 19]. In addition, phragmoplastin, a plant dynamin [20, 21], and KatAp, a plant kinesin [22], localize to the plane of cell division during plant cytokinesis. This observation suggests that these molecules may be used for vesicle transport and may be components of a cytokinesis execution mechanism that is conserved between plants and animals.

Taken together, these data suggest that secretion could be a common feature of cytokinesis in both plant and animal cells. To investigate what role secretion might play in animal cell cytokinesis, we isolated dividing *C. elegans* blastomeres [23, 24] and used BFA to inhibit secretion. Furrowing initiated normally in the treated blastomeres, but separation of the daughter cells did not occur and cleavage furrows ultimately regressed. In addition, BFA produced spindle alignment failures in asymmetrically dividing blastomeres. We have also observed the dynamics of membranes in control and BFA-inhibited blastomeres by using the membrane probe FM1-43. Using this probe, we found that there was a striking BFA-sensitive accumulation of membrane localized to the apex of the late cleavage furrow during the execution of the terminal phase of cytokinesis.

Results
Brefeldin A inhibits the terminal phases of cytokinesis in embryos and in isolated blastomeres
We used laser permeabilization and blastomere isolation techniques to study the effects of BFA on both intact embryos and isolated blastomeres [24–26]. BFA is a potent inhibitor of secretion and prevents the assembly of non-clathrin-coated vesicles from Golgi cisternae [27]. BFA acts by inhibiting the ADP ribosylation factor (ARF), a factor that is required for the assembly of vesicle coats and therefore for the budding of membrane-enclosed vesicles [28]. BFA also stimulates the ADP ribosylation of BARS proteins [29], which may normally exert a negative effect on Golgi tubulation. We selected embryos and blastomeres and placed them into culture media with and without BFA, then observed formation of the cleavage furrow by using 4D videomicroscopy [30].

We permeabilized the eggshells of early embryos by ablating 2–3 holes in the eggshell while the eggs were bathed in a culture medium containing 15 ug/ml BFA. The furrow completed during the initial division following exposure to BFA. However, although each of the second division furrows in the asynchronous population of blastomeres ingressed to apparent completion, they then regressed approximately 5–7 min later and gave rise to blastomeres with multiple nuclei (n = 14; Figure 1a). Control embryos that had been laser permeabilized in the absence of BFA continued to divide normally (data not shown).

We isolated blastomeres and placed them into culture medium containing 15 ug/ml BFA. The initial division following exposure to BFA completed, as with laser-permeabilized embryos. During the next division, a furrow was initiated at the correct time and appeared to go to completion; however, about 7 min after the furrow had apparently fully completed, the furrow regressed. The result was a binucleate cell (Figure 1c). The adjacent blastomere also attempted to complete cytokinesis but failed in the same manner. The two blastomeres continued to cycle and to go through multiple rounds of karyokinesis, with the spindle pole replicating normally at each cycle. At each cycle, furrows appeared between adjacent spindle poles; these furrows also always regressed. The observation that multiple furrows formed at these later stages indicated that the early cleavage failures were not due to limitations in the available area of plasma membrane. However, because of the known inhibitory effects of BFA on the secretory process, these experiments suggest that exocytosis is required for the completion of cytokinesis.

We noticed that the first division of the blastomeres always occurred normally in the BFA-treated cells. However, the second division always failed to complete the final stages of cytokinesis. By light microscopy, subsequent furrows appeared to complete, but since these eventually regressed, it seems that an essential step in cell division was in fact missing. We found that 15 ug/ml (0.0534 mM) BFA reliably produced failures in cytokinesis without affecting cell viability (n = 114). Higher concentrations of BFA (20 ug/ml or higher) led to cell cycle arrest and death. Lower concentrations of BFA did not produce any noticeable effects. The one-cell-cycle delay in the appearance of the BFA-induced defect in cytokinesis during the late stages of cytokinesis may be due to fast cell cycle progression (12–15 min) relative to the time of the onset of BFA action. Consistent with this notion, we found that when we placed one-cell embryos into culture medium with BFA after the completion of the meiotic divisions, the first cell division failed. This suggests that the relatively long first cell cycle following meiosis II (approximately 40 min) gave sufficient time for the BFA to act, whereas the 15–20 min cell cycle times of the early embryonic divisions did not. Furthermore, an embryo may well have sufficient preformed vesicles in the cytoplasm to accommodate the first cleavages that are seen in blastomeres at the two-cell stage or later. Subsequent cleavages might fail to complete in BFA-treated embryos because of

Figure 1
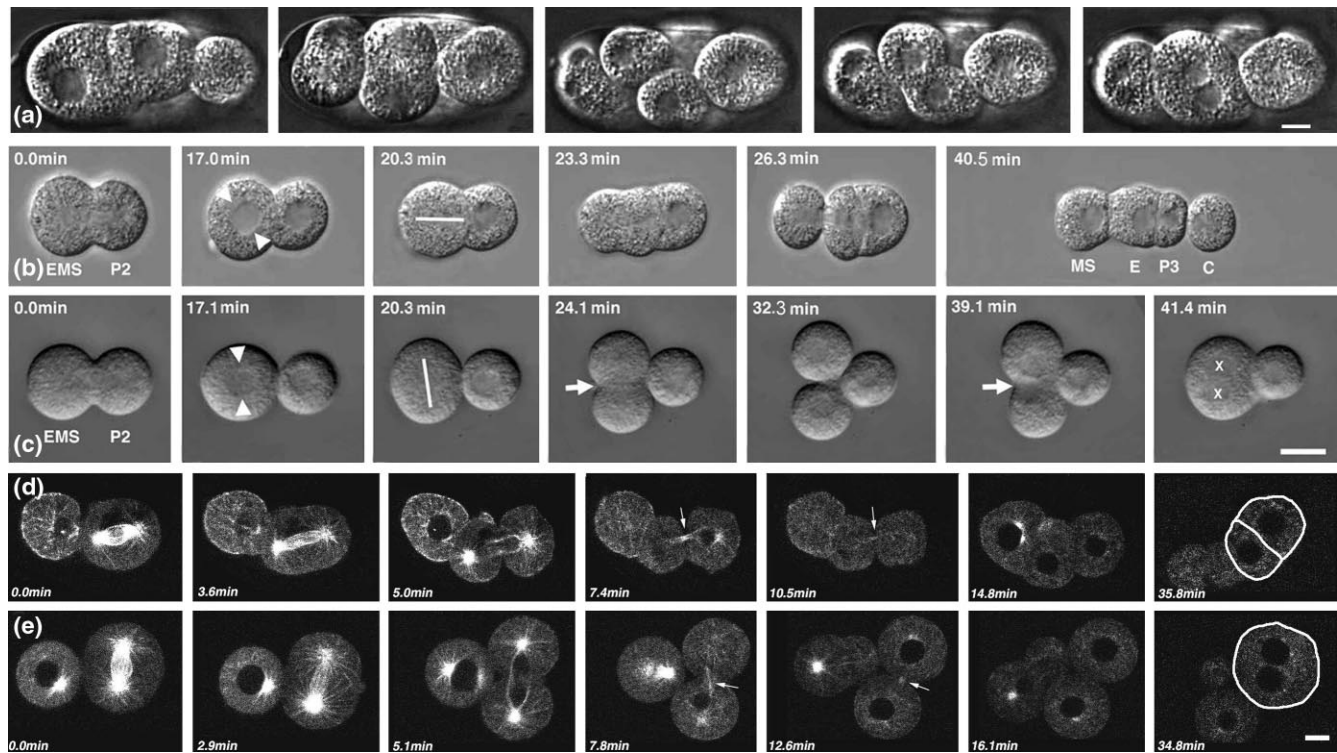
(a) Sequence taken from a 4D recording of an embryo that had been laser permeabilized in culture media containing 15 ug/ml BFA. The middle, in-focus cell was seen to undergo a cytokinesis that ultimately failed. All other blastomeres behaved in a similar way (cell divisions are asynchronous in *C. elegans* embryos). Adjacent panels are 4.0 min apart. The scale bar is 6 μm. **(b)** Isolated blastomeres in culture media with and without BFA addition. As a control, a P_1 blastomere was placed in culture media without BFA. At 0.0 min, P_1 is dividing into EMS and P_2. At 17.0 min, a centrosome-nucleus rotation event occurs in EMS towards P_2 (arrows mark centrosomes). At 20.3 min, the spindle in EMS aligns toward the point of contact with P_2 (line marks the spindle). At 23.3 min, EMS begins to divide asymmetrically. At 26.3 min, the final phase of division in EMS begins. At 40.5 min, EMS has completed division and given rise to MS and E (gut precursor). P_2 in the meantime has divided into P_3 and C. See also Movie 1 in the Supplementary material. **(c)** BFA-treated P_1 blastomere (15 ug/ml BFA). At 0.0 min, P_1 is dividing into EMS and P_2. At 17.1 min, the centrosome-nucleus complex in EMS does not rotate toward P_2 (arrows mark the centrosomes). At 20.3 min, the spindle in EMS is established on an improper axis. At 24.1 min, EMS begins to divide symmetrically. At 32.3 min, EMS appears to complete cytokinesis. At 39.1 min, the furrow in EMS regresses. At 41.4 min, EMS now has two nuclei. P_2 has also attempted to divide but has regressed (the other nucleus is out of focus). The scale bar is 5 μm. See also Movie 2 in the Supplementary material. **(d,e)** Microtubule dynamics in untreated and BFA-treated isolated blastomeres labeled with tubulin::GFP. (d) (0.0 min–35.8 min) Untreated blastomeres. Time points are as follows: 0.0 min, metaphase; 3.6 min, anaphase; 5.0 min, early telophase; 7.4 min, midbody formation (arrow); 10.5 min, midbody is still persisting (arrow); 14.8 min, midbody has disappeared; 35.8 min, interphase in both daughter cells (lines demark plasma membranes). See also Movie 3 in the Supplementary material. (e) (0.0 min–34.8 min) BFA-treated blastomeres. Time points are as follows: 0.0 min, metaphase; 2.9 min, anaphase; 5.1 min, early telophase; 7.8 min, midbody formation (arrow); 12.6 min, midbody is still persisting (arrow); 16.1 min, midbody has disappeared; 34.8 min, the furrow has regressed and the blastomere becomes multinucleate (lines demark plasma membranes). The scale bar is 5 μm. See also Movie 4 in the Supplementary material.

the depletion of the pool of vesicles. The late cytokinesis defects observed in our experiments suggest that there is a requirement for secretion even after the furrow has ingressed to its fullest extent. This in turn suggests that the final sealing of the intercellular canal requires localized membrane fusion events. Given data from previous work [11, 19], as well as the work presented here, cytokinesis may therefore involve two phases of new membrane insertion and fusion events: initially, providing new membrane for furrow ingression [11, 19, 31] and, finally, adding membrane locally in the spindle midzone region to break

the intercellular bridge and seal the newly formed daughter cells (this study).

The spindle midzone and midbody microtubules are normal in BFA-treated blastomeres

In order to assess whether BFA affected the spindle midzone structure or midbody (a structure known to be required for the completion of cytokinesis [2–5]), we visualized microtubule dynamics in blastomeres expressing tubulin::GFP [32]. Untreated and BFA-treated tubulin::GFP-expressing blastomeres were placed into culture me-

dia and observed by multiphoton microscopy. In untreated blastomeres, the time from furrow ingression to the disappearance of the midbody was 10.95 ± 1.15 min (n = 6). In that time, the midbody persisted for 5.85 ± 1.05 min (Figure 1d and, in the Supplementary material available with this article on the internet, Movie 3). This time period corresponds to the period in which we observed the accumulation of membrane in FM1-43-labeled blastomeres (see Figure 4a). In BFA-treated blastomeres, the time from furrow ingression to the disappearance of the midbody was 11.15 ± 0.35 min (n = 9). The midbody persisted for 6.3 ± 1.2 min in these treated blastomeres (Figure 1e and, in the Supplementary material, Movie 4). Therefore, BFA has no visible effect on the midzone microtubules in the time period in which one would normally observe membrane accumulation (see Figure 4).

Inhibition of *rab-11* expression by RNAi produces similar effects to those of BFA in early embryos

In order to assess whether the effects that we observed with BFA treatment were, in fact, due to the inhibition of secretion, we investigated an alternative way of inhibiting secretion: using RNAi to suppress the expression of some of the *rab* GTPases. We suppressed expression of *rab-8* and *rab-11* (two components of the secretory pathway involved in Golgi-to-membrane targeting [33–35]) by injecting double-stranded RNA synthesized from the entire *rab-8* or *rab-11* coding region. We observed animals and embryos 16–28 hr postinjection. Suppressing the expression of *rab*-8 produced severe deformation of the ovaries and thus prevented any eggs from being produced (data not shown). Suppressing *rab-11* expression also gave rise to defects in the syncytial germ cell in the ovary (Figure 2g,h). In this case, the nuclei of the syncytial germ cell were seen throughout the cell rather than in their normal configuration at the periphery. The defects seen with *rab-11* RNAi were not as severe as with *rab-8*, and fertilized eggs were produced. The cellularization defects that we observed were similar to those seen in BFA-treated *Drosophila* embryos [31]. Polar-body formation was also inhibited, as shown by additional nuclei in the zygote, P_0. In P_0, the furrow appeared to complete; however, 7–9 min into the second cell cycle the furrow regressed (Figure 2d). This regression suggests that the final stages of cytokinesis require Rab-11. In embryos observed 20–28 hr postinjection or later, the furrow ingressed approximately 1/2–3/4 of the way into the cell and then regressed (n = 15; Figure 2b). These data suggest that Rab-11 may also be required for supplying the extra membrane required for furrowing. The RNAi suppression of Rab expression starts to act in the syncytial germ cell, whereas the BFA was applied after fertilization. This timing difference probably explains why no partial ingressions were observed in the BFA-treated embryos. Membrane insertion at the tip of the advancing furrow has been seen in *Xenopus* [36] and requires microtubules [37]; these observations

indicate that targeted secretion is involved at all stages of furrow ingression, not unlike the situation in plants. This is consistent with the varying degrees of furrow invagination that are observed in *rab-11* RNAi-treated blastomeres.

Spindle alignment defects are observed in BFA-treated blastomeres

During the course of the isolated blastomere experiments, we noticed that certain blastomeres, when treated with BFA, exhibited spindle alignment defects. In the intact embryo, a P_1 blastomere divides asymmetrically and gives rise to a larger cell, EMS, and a smaller cell, P_2 [38]. The P_2 blastomere induces EMS to divide asymmetrically by causing the spindle to be aligned with one pole adjacent to the point of contact (Figure 1b) and a gut precursor, E, to be produced adjacent to P_2. In the absence of an inducing signal from P_2, the spindle does not align in the normal manner, and the E blastomere fate is not produced [26]. The interaction between P_2 and EMS in the four-cell embryo has been well characterized [26] and involves WNT signaling pathways [39, 40]. In BFA-treated blastomeres, the centrosome-nucleus complex did not rotate in EMS, and the spindle set up in the wrong orientation (Figure 1c, 20.3 min; 23/26 EMS blastomeres failed to align their spindles). The EMS cleavages were symmetrical, and all eventually failed after full furrow ingression. The P_2 spindle orientation, however, occurred in the proper orientation (8/9 P_2 blastomeres) as judged from tubulin::GFP data (data not shown). This finding suggests that spindle orientation does not require secretion in the case of the P lineage.

Internal membrane dynamics in *C. elegans* embryos

We observed internal membrane dynamics in the early embryo by using a Bodipy BFA probe. Bodipy BFA is an inactive form of brefeldin A conjugated to a Bodipy fluorophore. It labels Golgi and ER in mammalian cells and colocalizes with a NBD-ceramide probe [41]. The addition of unlabeled BFA with the Bodipy BFA probe did not produce any localized fluorescence. Bodipy alone does not label internal membranes [41]. The endomembrane system, as visualized with Bodipy BFA, was seen to consist of a heterogeneous cloud of vesicles distributed throughout the embryo (Figure 3a). Other ER probes, such as DiI, revealed a similar pattern (A. Badrinath, personal communication).

The dynamic behavior of the Bodipy BFA-labeled vesicles can be seen in Movie 5 in the Supplementary material. At the moment the egg and sperm pronuclei meet, relatively large vesicles (approximately 0.3–1.3 μm) were seen aggregating in the vicinity of the astral microtubules (Figure 3b). Vesicles of this size have been observed trafficking and fusing with the plasma membrane in mammalian cells [42]. The spindle body together with the

Figure 2

rab-11, *rab-8*, and wild-type RNAi Nomarski sequences. **(a)** Wild-type P$_0$ sequence from furrow ingression thru interphase in the 2-cell stage. **(b)** Furrow ingression through furrow regression at the 2-cell stage in the *rab-11* sequence (note that the furrow comes 3/4 of the way into the cell and then regresses). **(c)** Three-cell stage through four-cell stage in the wild type. The furrow is completing in the posterior blastomeres (in this case, AB daughters). **(d)** The 3-cell stage through the 4-cell in *rab-11*. The posterior blastomeres have completed, but they retract as time progresses. **(e)** Top focal plane of a wild-type gonad (control, water injected; note the normal organization of germ nuclei that was observed). **(f)** Middle focal plane of a wild-type gonad; Notice the nuclei are only situated at the periphery of the gonad. **(g)** Top focal plane of a *rab-11* gonad. **(h)** Middle focal plane of a *rab-11* RNAi-treated gonad. Nuclei are found in the periphery of the gonad as well as in ectopic locations in the central core of the rachis. The scale bar is 10 μm.
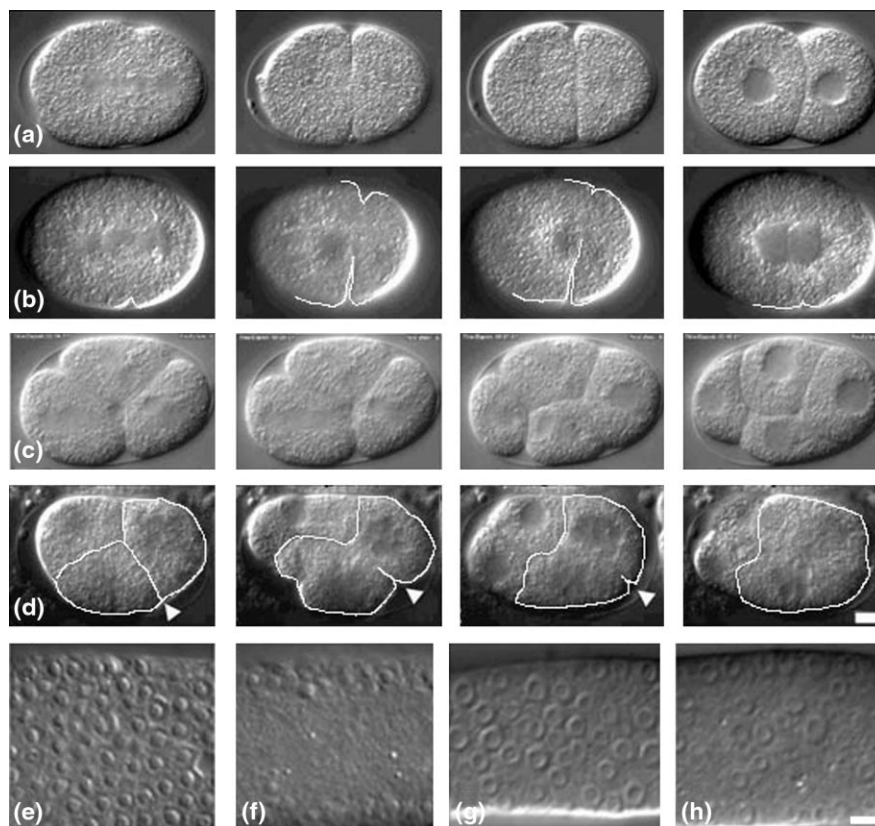
region around the centrosomes exhibited a diffuse fluorescence presumably emanating from subresolution vesicles. The centrosome excluded this source of signal. During metaphase, the chromatin and adjacent spindle also excluded these vesicles, although subresolution vesicles were still present around the centrosomes (Figure 3c). Upon anaphase onset, we observed diffuse, small-vesicle staining that became localized to the spindle midzone region (Figure 3d). This staining was conspicuous from anaphase through telophase and eventually diminished in intensity after this time. During late telophase, we observed larger vesicles moving parallel to midzone microtubules toward the equatorial plane (Figure 3e). After the furrow ingressed, movement along the axis of the intercellular canal was observed (see Movie 5). The exact role and function of these vesicles remains unclear at this time. However, these observations indicate that large and subresolution vesicles localize along the spindle midzone in the vicinity of the ingressing furrow during the terminal phase of cytokinesis.

Plasma membrane dynamics during cytokinesis

To visualize plasma membrane dynamics during cytokinesis in isolated blastomeres and laser-permeabilized embryos, we used the membrane probe FM1-43 (Molecular Probes). This styrylpyridinium dye is a nontoxic, water-soluble dye, believed to insert into the outer leaflet of the surface membrane, where it becomes intensely fluorescent [43]. We followed the dynamics of the plasma membrane in cleaving cells by using multiphoton time-lapse microscopy [44, 45].

Following the completion of an ingressed furrow, we observed a pronounced accumulation of membrane occurring at the leading edge of the ingressed furrow that forms the intercellular canal (n = 13; Figure 4a, 4–12 min). This accumulation persisted until 5–7 min into the next cell cycle. Prior to the next division, it appeared that the cell division remnant was internalized along with this bolus of accumulated membrane and moved toward a centrosome (n = 4; Figure 4a, 16.0 min).

Four-dimensional, multiphoton membrane-imaging experiments showed that membrane accumulates at intercellular canals between all blastomeres in developing embryos (n = 9) or in isolated blastomeres (n = 31) (Figure 4b and, in the Supplementary material, Movie 7). Higher magnification of furrowing events in these embryos revealed a progressive accumulation of membrane (Figure 4c and Movie 8).

When we treated blastomeres with BFA, we found that

Figure 3
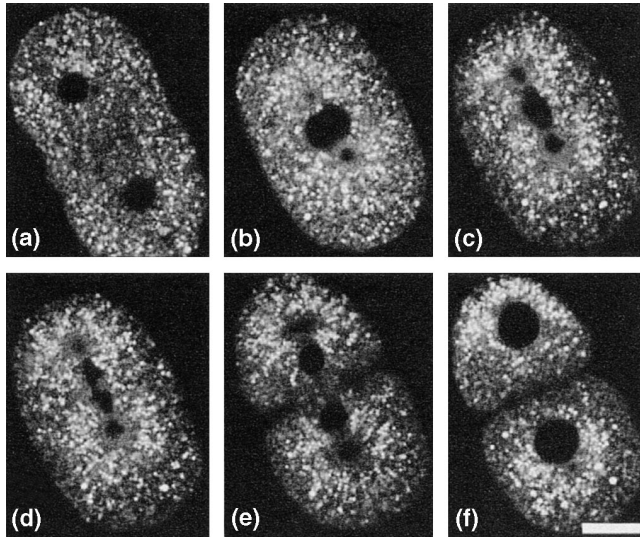
Internal membrane dynamics in early embryos labeled with Bodipy BFA. The sequence of 2D multiphoton images begins prior to pronuclear migration and ends after cleavage. Vesicles are fairly uniformly dispersed before **(a)** pronuclear migration. **(b)** At the time the pronuclei meet, vesicles begin to aggregate around the pronuclei. From the movies it can be seen that vesicles are moving toward the centrosome in straight lines, presumably along astral microtubules, and can be seen aggregating in **(e)**. Note the difference in the nature of the staining around the centrosome and the cytoplasm. The pericentrosomal region excludes larger vesicles, whereas the centrosomes and nucleus exclude all membrane staining. **(c)** In metaphase, the entire spindle midzone excludes vesicular staining. **(d)** Upon anaphase onset, the spindle midzone fills in with diffuse membrane staining, probably from small vesicles. (e) Late in anaphase-telophase, large vesicles can been seen trafficking toward and past the equatorial region (Movie 5 in the Supplementary material). **(f)** Cleavage has completed. The scale bar is 12.5 μm.

this accumulation did not occur (Figure 5 and Movie 9). The furrow ingressed, appeared to complete, and maintained this configuration for approximately 4–7 min (n = 52, similar to the situation for untreated blastomeres). However, no accumulation of membrane was observed at the intercellular canal, and the furrow subsequently completely regressed after this period (Figure 5, 4.5–7 min). The failed blastomeres attempted cleavage again at the next cell cycle; they produced multiple furrows but again failed, and this finding suggests that there was sufficient membrane available for invagination. The results suggest that membrane accumulation at the persisting intercellular canal could be required for the completion of cytokinesis.

Discussion

Traditionally, the mechanisms underlying cytokinesis in animal cells have been considered different from those used by plant cells. However, recent work in the field, together with work presented in this paper, supports a model of cytokinesis that is similar in plant and animal cells. For example, actin-myosin rings and a requirement for secretion are common to both animal and plant cells [14, 18, 19, 31, 46]. The work described in this paper suggests, however, that secretion is required not only for initial furrowing events, but also during the terminal stages that finally separates the two daughter cells from each other.

Using 4D-multiphoton microscopy, we observed FM1–43-labeled membrane accumulating immediately after the furrow became fully ingressed. Such accumulation could be caused by Golgi-derived vesicles that are targeted to the apex of the cleavage furrow, where they exocytose. Alternatively, membrane could accumulate by flowing down the apex of the furrow into the tip. When a cell cleaves, the surface area has to increase, which implies that new plasma membrane has to be inserted. We found that BFA treatment did not inhibit furrowing. Indeed, following a cytokinesis failure, multiple furrows formed between all pairs of centrosomes. These observations strongly suggest that lack of a sufficient area of plasma membrane is not the reason why the terminal phase of cytokinesis fails following BFA treatment. Possibly, BFA is having differential effects on secretion and is only inhibiting targeted secretion in the vicinity of the spindle midzone. However, perhaps a more likely explanation is that the plasma membrane of the cells that we study have sufficient excess membrane in the form of ruffles or other surface irregularities for the increase in surface area during cytokinesis to be accommodated. This would imply that it is the BFA-induced failure of exocytosis after the furrow is fully ingressed that is causing cytokinesis to fail.

There are interesting parallels between the terminal phase of cytokinesis and the response of cells to wounding. Both may involve membrane breakage and resealing. Data have been presented that suggest that membrane resealing following wounding is accomplished by a Ca^{2+}-dependent exocytosis. Furthermore, the response to wounding is facilitated by previous wounding in a BFA-dependent manner [47], and this finding implies that, at least for facilitated repair, the exocytosis of Golgi-derived vesicles is required.

Secretion and spindle alignment

In BFA-treated EMS and P_2 blastomeres, spindle alignment is inhibited. Dynein/dynactin complexes are required for spindle alignment and localize to cortical sites that correspond to cell division remnants [48, 49]. A possible interpretation of the failure of rotational alignment in brefeldin A-treated blastomeres is that vesicular transport is required for the localization of dynactin to cortical microtubule attachment sites that correspond to previous cell division remnants. Similar effects of BFA on cleavage plane orientation have been observed in *Fucus*, in which

Figure 4
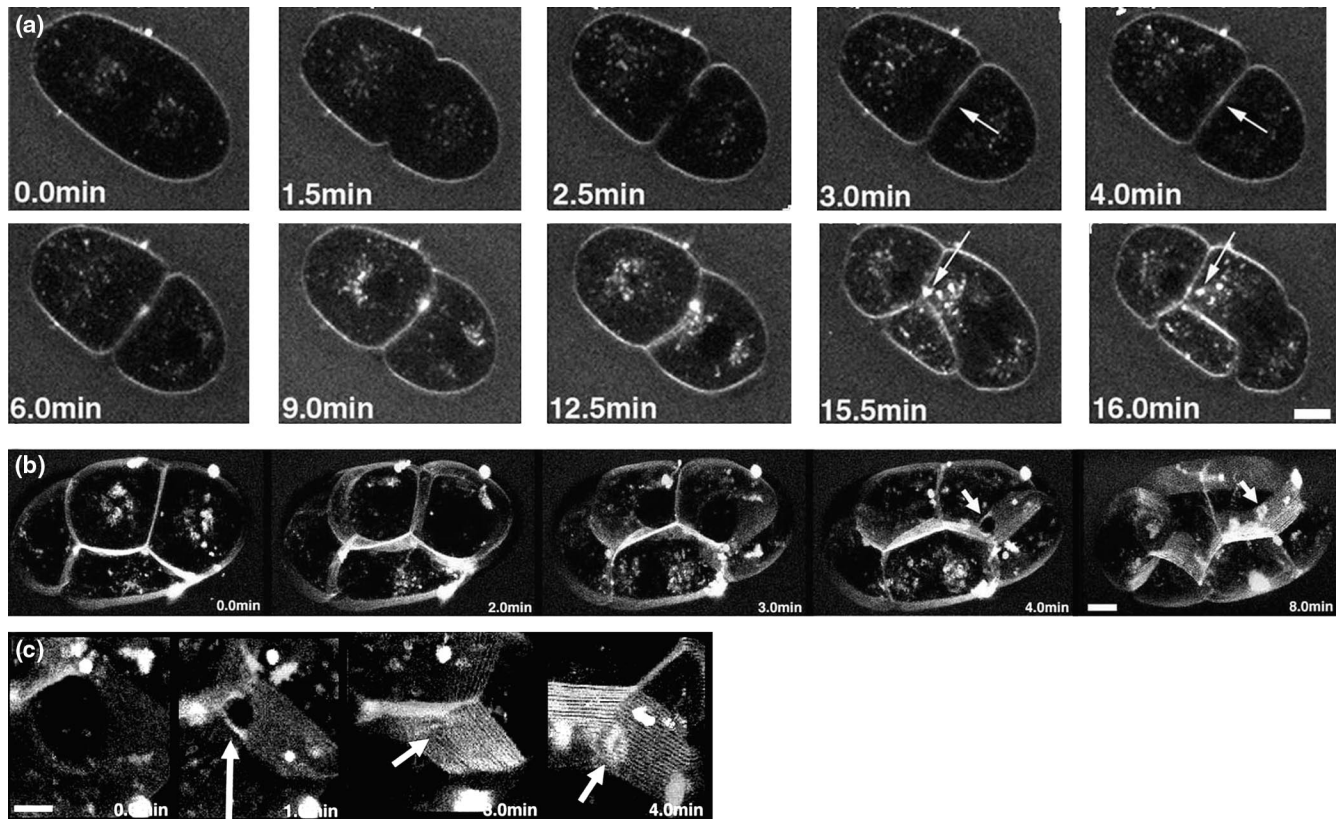
(a) Plasma membrane dynamics in the early embryo. The multiphoton time course of a single focal plane taken from an embryo labeled with FM1-43 is shown (2D images). Furrow invagination began at 1.5 min and appears to have completed at 3.0 min. Accumulation of membrane at the intercellular canal occurred after furrow completion from around 4.0 to 12.5 min. Note how the intensity of the staining in the spindle midzone region increases over time. At 16 min, the accumulated membrane appeared to become dissociated from the plasma membrane and internalized. The scale bar is 5 μm. See also Movie 6 in the Supplementary material. **(b)** Four-dimensional membrane dynamics in the embryo. The multiphoton time course of an embryo labeled with FM1-43 is shown (3D images). Images show a rotated 3D projection. The sequence shows the larger blastomeres (ABa and ABp) located on the top right as they divided (mitotic spindles are normal to the projection plane). The embryo is in interphase at 0.0 min. By 2.0 min, the furrows begin to invaginate. After 3.0 min, furrows are 3/4 complete. An arrow identifies a late furrow in one of the blastomeres after 4.0 min. The other furrow was out of focus. Four minutes past the previous time point (at 8.0 min.), an accumulation of membrane at the late furrow is observed (arrow). The scale bar is 5 μm. See also Movie 7 in the Supplementary material. **(c)** Magnified view of the terminal phase of cytokinesis in a developing blastomere. The sequence shows a series of rotated 3D projections from a 4D data set. Striations are individual optical sections. At 0.0 min, furrow initiation in a blastomere is shown. By 1.0 min, the furrow was near completion. After 3.0 min the furrow appeared complete, but a minute later (at 4.0 min) extra membrane had accumulated where the furrow had completed (arrow). The scale bar is 3.4 μm. See also Movie 8 in the Supplementary material.

Golgi-derived material (GDM) is required at cortical sites prior to axis orientation [50]. The midbody in animal cells could therefore be a spindle-derived scaffold for various targeted proteins involved in cell separation events as well as spindle alignment events (Figure 6).

It is possible that kinesin molecules bound to vesicles could move dynactin/dynein (also bound to these vesicles) to plus ends of microtubules that reside in the intercellular canal. Alternatively, WNT signals or their receptors may be prevented from being transported to the cell surface if secretion is being blocked by BFA, as several of the *mom* genes (WNT pathway genes in *C. elegans*) are known to be required for proper spindle alignment [51].

Secretion, motor molecules, and cytokinesis
The involvement of BFA-sensitive pathways (this study; [31]) and syntaxins [19] in cytokinesis raises the possibility that other evolutionarily conserved molecules involved in secretion, such as the dynamins or Rab GTPases, might be necessary during animal cytokinesis, as seen in plants. Recent studies of Rabkinesin 6 [52], XKLP3 [53], and a plant kinesin, KatAp [22], suggest that kinesins are also involved in targeted secretion. Inhibition of kinesin or
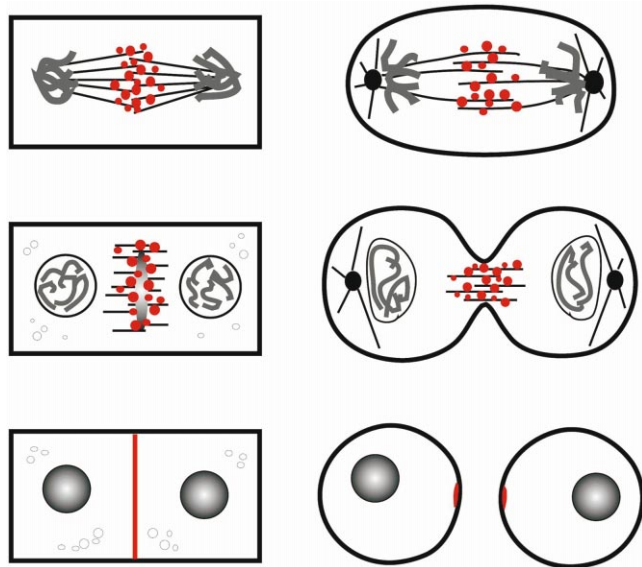
Figure 5
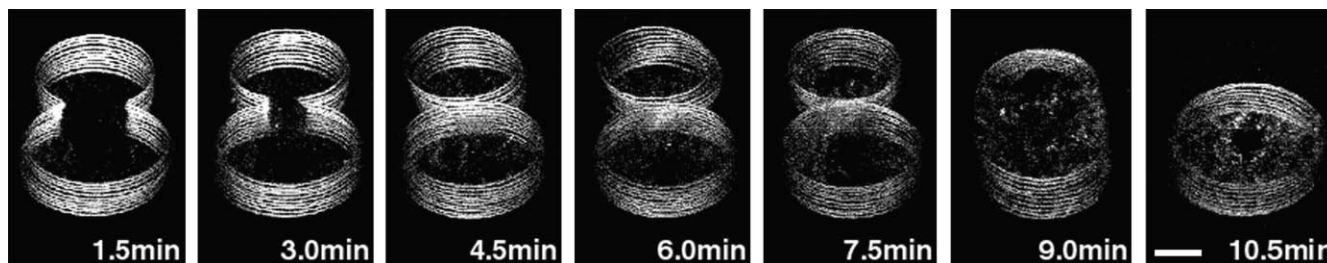
Membrane dynamics in an isolated blastomere treated with BFA. The multiphoton time course of a P_0 blastomere labeled with FM1-43 in the presence of BFA is shown. The figure shows a sequence of 3D projections of a thick axial slice taken through the dividing cell. At the 1.5 min time point, the furrow had invaginated. By 3.0 min, the furrow had almost completed. During a period from 4.5 min to 7.5 min, the furrow stayed fully ingressed. No membrane accumulation can be seen in the vicinity of the late cleavage furrow. However, one minute after this period the furrow had regressed (9.0 min). The furrow remained ingressed for 5.5 min before regressing in the BFA-treated embryo. This time corresponds to the time in which membrane accumulation would have normally occurred in untreated blastomeres; however, no accumulation was seen, and ultimately, cytokinesis failed. At 10.5 min the cleavage furrow had completely regressed. The blastomere continued to initiate cleavage and furrows completed again, but these also failed (data not shown). The scale bar is 14 μm. See also Movie 9 in the Supplementary material.

myosin function has also been shown to prevent membrane resealing and delivery to sites of membrane disruption [54, 55]. Inhibition of Rabkinesin 6/Rab6-KIFL has recently been found to produce cytokinesis defects in HeLa cells [56], and this finding suggests that targeting pathways are indeed involved in secretion and that these pathways are involved in cytokinesis as well.

Kinesins, such as KLP3A [57] and ZEN-4/CeMKLP1 [6, 7], have been found localized to spindle midzone microtubules and are also necessary for the completion of cytokinesis. The spindle midzone fails to assemble in *zen-4* mutants [6, 7]. The RhoGAP CYK-4 also interacts with ZEN-4 [58], and this finding suggests a cooperative interaction during the assembly and maintenance of the spindle midzone. Future molecular and genetic studies may provide clues to the role of microtubule-based molecular motors and associated regulatory proteins in midzone assembly and vesicle targeting during cytokinesis.

Recent evidence suggests that the motor molecules that are used in vesicle transport in neurons depend on the distance the vesicles must travel [59, 60]. The microtubule network is thought to be used primarily for long-range vesicle transport and to require microtubule-based motors, such as kinesins. The actin network, however, is used for short-range transport and motors such as myosin-Va [59]. In *S. cerevisiae*, it is known that vesicles are transported along actin cables toward the mother-bud neck and that this transport requires Myosin Va [61–63]. In plants, both the microtubule and actin cytoskeletons are crucial for normal cell division [1, 64]. Recent evidence of short-range, actin-based vesicle movement has been observed in *Xenopus* extracts and suggests that vesicle transport may be mediated with the aid of treadmilling actin tails [65]. Whether these mechanisms are required during cytokinesis is unclear. Since actin is locally enriched in the terminal furrow in animal cells [49, 66, 67],

Figure 6

Targeted exocytosis is required in both plant and animal cytokinesis. Plant cytokinesis is depicted on the left and animal cytokinesis on the right. The model proposes that vesicles (circles) traffic along microtubules toward the equatorial plane of the cell in both plant and animal cells. In plants, vesicles are transported along the microtubules of the phragmoplast and ultimately fuse at the equatorial plane forming the cell plate between the daughter cells. In animal cells, vesicles are transported along the microtubules of the residual body of the mitotic apparatus to the midzone, where they fuse and seal off the intercellular canal and thus separate the daughter cells.

Model for vesicle fusion in sealing off the intercellular canal. The sequence shows events that may occur at the apex of the furrow. Here, progressive vesicle fusion in the vicinity of the persisting intercellular canal forms finger-like projections that fuse with the membrane from the opposite side of the furrow. Cell separation is then complete.
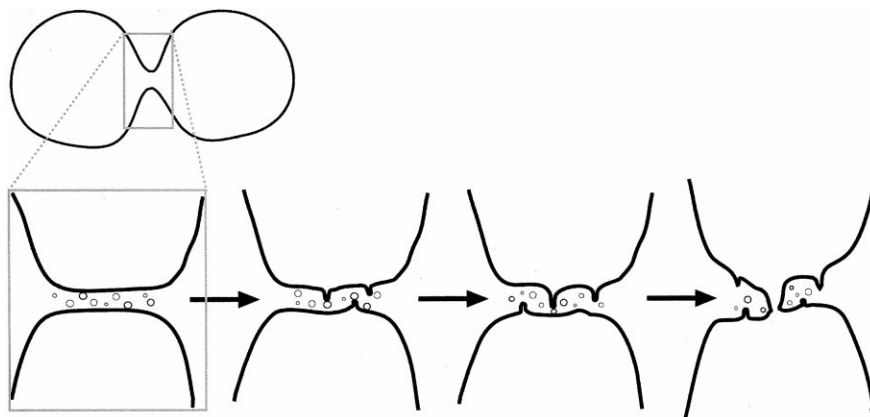
it is possible that actin may play a role in localized movements of vesicles between the midbody and plasma membrane during the terminal phase of cytokinesis.

Membrane accumulation at terminal furrows

Membrane accumulates at the intercellular canal after furrow completion. The increase in membrane labeling seen at the apex of the late cleavage furrow with an extracellular membrane probe is probably due to extensive, localized plasma membrane ruffling caused by the local insertion of new membrane. Our observations suggest that this localized accumulation is required for breaking and resealing the intercellular canal during the terminal phase of cytokinesis. It has been observed that blastomeres cannot be separated until 5 min after cleavage [26]; (A.R.S., unpublished observation); perhaps this time reflects the time required to break and reseal the intercellular canal. We have shown that BFA-treated blastomeres do not accumulate membrane within this time frame and that they suffer cytokinesis failures, and this finding indicates that membrane-targeting mechanisms are necessary during the late stage of cytokinesis in a process similar to that of plants. Internal, BFA binding vesicles aggregate along astral and spindle microtubules prior to cytokinesis. Movement of vesicles along the spindle midzone toward the equatorial plane was observed, although membrane fusion events could not be seen because they are beyond optical resolution limits in this system. Because of the impenetrable eggshell and rapid cell cycle, electron microscopy of cell division events in early *C. elegans* embryos has proven to be difficult, and the ultrastructure of membrane events during the completion of cytokinesis in *C. elegans* is at yet unknown. However, electron microscopy of staged spindle midzones may well shed light on the mechanisms that control the final phase of cytokinesis.

The late stages of cytokinesis

In several organisms, including *C. elegans*, a number of proteins have been shown to be required for the late stages of cytokinesis. INCENPs/ICP-1/ICP-2 [68, 69], ZEN-4/CeMKLP1/CHO1/pavarotti/ [6, 7, 70, 71], KLP3A [57], the formin gene (CYK-1) [72], the aurora kinase (AIR-2) [8, 69], and a RhoGAP (CYK-4) [58] are all required for the late stages of cytokinesis. Their exact role in the final stages of cytokinesis is unclear. Their mutant phenotypes suggest that these proteins are required for the maintenance of the contractile ring, formation of the spindle midzone structure, or both. We suggest that these proteins are required, not for the actual pinching off of membrane, but for the stabilization of the cytokinetic ring and/or the maintenance of the structural integrity of the spindle midzone. We propose that these conditions are necessary for targeting BFA-sensitive vesicles to the region of the intercellular canal and allow vesicles to fuse into a miniature cell plate that would allow the two cells to separate (Figure 7). Furthermore, we propose that the spindle midzone of animal cells is functionally analogous to the plant phragmoplast along which BFA-sensitive vesicles are transported to the equatorial plane, where they fuse to form the cell plate.

Materials and methods

Nematode culture
N2 strains were kept at 20ºC and cultured as described by Brenner [73]. The tubulin::GFP (WH204) strain was cultured at 25°C [32].

Examination of embryos and blastomeres
Embryos and blastomeres were examined by light microscopy with Nomarski differential interference contrast microscopy. Embryos were mounted on a 3% agarose pad in M9, and a 22 mm × 22 mm coverslip was placed on top and sealed with Vaseline. Blastomeres were mounted on subbed slides [49] in culture media, covered with a coverslip with grease feet, and sealed with silicon oil (Sigma, M-6884). Development was recorded with a Hamamatsu model C2400 video camera and 4D videomicroscopy [30].

Blastomere isolation and BFA concentration
Blastomeres were isolated by techniques used by Goldstein [26], placed in blastomere culture media [74] with or without 15 ug/ml (0.0534 mM) of BFA (Sigma, B-7651) [50], and observed with 4D videomicroscopy.

Laser ablation techniques
Embryos were mounted on a 2% polylysine-coated coverslip with grease feet, placed on a slide, and sealed with silicon oil. Laser ablation of the eggshell (in 2–3 places) was performed by techniques used by Hyman [25] and by Mohler et al. [75]. BFA (15 ug/ul) was added to culture media before laser ablation.

RNAi injections
RNA (sense and antisense) from the relevant *C. elegans* cDNA clone was synthesized with the MEGAscript In Vitro Transcription Kit (Ambion). Sense and antisense RNA was resuspended in DEPC-treated water at a concentration of 3.5–5 mg/ml and mixed into the same tube. Injection into the gonads of wild-type hermaphrodites was performed as described by Mello et al. [76]. The following *C. elegans* mRNAs were injected into the hermaphrodite gonads: rab-11 cDNA (F53G12.1/yk51h1) and rab-8 (D10B7.4/yk451h3 and yk282h8). The dsRNA that was made covered the entire rab-11 and rab-8 coding regions. Water was used as a control (no defects were observed). Other rab proteins have not been shown to produce early embryonic defects in *C. elegans* [77]. The phenotypes of the F1 embryos were examined with Nomarski 4D microscopy [30].

Membrane visualization and multiphoton microscopy
FM1-43 (Molecular Probes, T-3163) was used for the visualization of membranes during mitosis. Bodipy BFA (Molecular Probes, B-7447) was used for the visualization of cytoplasmic vesicles. We used 0.01 mg/ml FM1-43 and 15 ug/ml Bodipy BFA in blastomere culture medium [74]. Selected embryos or blastomeres were isolated and mounted in culture media containing FM1-43 or Bodipy BFA with or without BFA (15 ug/ml) diluted in culture media. Bodipy BFA with BFA in the culture media did not produce any localized fluorescence (anticipated results; Molecular Probes); we used this as a control (data not shown). Embryos or blastomeres were placed on a polylysine-subbed slide. A coverslip with grease feet was placed on top, diluted media were added, and the slides were then sealed with silicon oil. A multiphoton microscope was used for capturing images at the Integrated Microscopy Resource, University of Wisconsin-Madison, as described by Mohler et al. [45].

Image processing
Images were processed with NIH Image 1.61 b7 and then Adobe PhotoShop 5.5 (Adobe Systems, Mountain View, California).

Supplementary material
Animated versions of Figures 1b–e, 3, 4a–c, and 5 (see Movies 1–9) are available with this article on the internet at http://images.cellpress.com/supmat/supmatin.htm.

References
1. Staehelin LA, Hepler PK: **Cytokinesis in higher plants**. *Cell* 1996, **84:**821-824.
2. Rappaport R: *Cytokinesis in Animal Cells*. New York: Cambridge University Press; 1996.
3. Mullins JM, McIntosh JR: **Isolation and initial characterization of the mammalian midbody**. *J Cell Biol* 1982, **94:**654-661.
4. Sanger JM, Pochapin MB, Sanger JW: **Midbody sealing after cytokinesis in embryos of the sea urchin *Arabacia punctulata***. *Cell Tissue Res* 1985, **240:**287-292.
5. Wheatley SP, Wang Y: **Midzone microtubule bundles are continuously required for cytokinesis in cultured epithelial cells**. *J Cell Biol* 1996, **135:**981-989.
6. Raich WB, Moran AN, Rothman JH, Hardin J: **Cytokinesis and midzone microtubule organization in *Caenorhabditis elegans* require the kinesin-like protein ZEN-4**. *Mol Biol Cell* 1998, **9:**2037-2049.
7. Powers J, Bossinger O, Rose D, Strome S, Saxton W: **A nematode kinesin required for cleavage furrow advancement**. *Curr Biol* 1998, **8:**1133-1136.
8. Schumacher JM, Golden A, Donovan PJ: **AIR-2: an Aurora/Ipl1-related protein kinase associated with chromosomes and midbody microtubules is required for polar body extrusion and cytokinesis in *Caenorhabditis elegans* embryos**. *J Cell Biol* 1998, **143:**1635-1646.
9. O'Connell KF, Leys CM, White JG: **A genetic screen for temperature-sensitive cell-division mutants of *Caenorhabditis elegans***. *Genetics* 1998, **149:**1303-1321.
10. Piel M, Nordberg J, Euteneuer U, Bornens M: **Centrosome-dependent exit of cytokinesis in animal cells**. *Science* 2001, **291:**1550-1553.
11. Danilchik MV, Funk WC, Brown EE, Larkin K: **Requirement for microtubules in new membrane formation during cytokinesis of *Xenopus* embryos**. *Dev Biol* 1998, **194:**47-60.
12. Sawai T, Yomota A: **Cleavage plane determination in amphibian eggs**. *Ann N Y Acad Sci* 1990, **582:**40-49.
13. Kalthschmidt JA, Davidson CM, Brown NH, Brand AH: **Rotation and asymmetry of the mitotic spindle direct asymmetric cell division in the developing central nervous system**. *Nature Cell Biology* 2000, **2:**7-12.
14. Yasuhara H, Sonobe S, Shibaoka H: **Effects of brefeldin A on the formation of the cell plate in tobacco BY-2 cells**. *Eur J Cell Biol* 1995, **66:**274-281.
15. Lukowitz W, Mayer U, Jurgens G: **Cytokinesis in the *Arabidopsis* embryo involves the syntaxin-related KNOLLE gene product**. *Cell* 1996, **84:**61-71.
16. Lauber MH, Waizenegger I, Steinmann T, Schwarz H, Mayer U, Hwang I, et al.: **The *Arabidopsis* KNOLLE protein is a cytokinesis-specific syntaxin**. *J Cell Biol* 1997, **139:**1485-1493.
17. Burgess RW, Deitcher DL, Schwarz TL: **The synaptic protein syntaxin1 is required for cellularization of *Drosophila* embryos**. *J Cell Biol* 1997, **138:**861-875.
18. Conner SD, Wessel GM: **Syntaxin is required for cell division**. *Mol Biol Cell* 1999, **10:**2735-2743.
19. Jantsch-Plunger V, Glotzer M: **Depletion of syntaxins in the early *Caenorhabditis elegans* embryo reveals a role for membrane fusion events in cytokinesis**. *Curr Biol* 1999, **9:**738-745.
20. Gu X, Verma DP: **Phragmoplastin, a dynamin-like protein associated with cell plate formation in plants**. *Embo J* 1996, **15:**695-704.
21. Gu X, Verma DP: **Dynamics of phragmoplastin in living cells during cell plate formation and uncoupling of cell elongation from the plane of cell division**. *Plant Cell* 1997, **9:**157-169.
22. Liu B, Cyr RJ, Palevitz BA: **A kinesin-like protein, KatAp, in the cells of arabidopsis and other plants**. *Plant Cell* 1996, **8:**119-132.
23. Hyman AA, White JG: **Determination of cell division axes in the early embryogenesis of *Caenorhabditis elegans***. *J Cell Biol* 1987, **105:**2123-2135.
24. Edgar L: **Blastomere culture and analysis.** In *Caenorhabditis elegans: Modern Biological Analysis of an Organism*. Edited by Epstein HF and Shakes D. San Diego: Academic Press; 1995:303-321.
25. Hyman AA: **Centrosome movement in the early divisions of *Caenorhabditis elegans*: a cortical site determining centrosome position**. *J Cell Biol* 1989, **109:**1185-1193.
26. Goldstein B: **Cell contacts orient some cell division axes in the *Caenorhabditis elegans* embryo**. *J Cell Biol* 1995, **129:**1071-1080.
27. Orci L, Tagaya M, Amherdt M, Perrelet A, Donaldson JG, Lippincott-Schwartz J, et al.: **Brefeldin A, a drug that blocks secretion, prevents the assembly of non-clathrin-coated buds on Golgi cisternae**. *Cell* 1991, **64:**1183-1195.
28. Helms JB, Rothman JE: **Inhibition by brefeldin A of a Golgi membrane enzyme that catalyses exchange of guanine nucleotide bound to ARF**. *Nature* 1992, **360:**352-354.
29. Spano S, Silletta MG, Colanzi A, Alberti S, Fiucci G, Valente C, et

al.: **Molecular cloning and functional characterization of brefeldin A-ADP-ribosylated substrate. A novel protein involved in the maintenance of the Golgi structure.** *J Biol Chem* 1999, **274:**17705-17710.

30. Thomas C, DeVries P, Hardin J, White J: **Four-dimensional imaging: computer visualization of 3D movements in living specimens.** *Science* 1996, **273:**603-607.

31. Sisson JC, Field C, Ventura R, Royou A, Sullivan W: **Lava lamp, a novel peripheral Golgi protein, is required for *Drosophila melanogaster* cellularization.** *J Cell Biol* 2000, **151:**905-918.

32. Strome S, Powers J, Dunn M, Reese K, Malone C, White JG, *et al.*: **Spindle dynamics and the role of gamma-tubulin in early *C. elegans* embryos.** *Mol Biol Cell* 2001, in press.

33. Chen W, Feng Y, Chen D, Wandinger-Ness A: **Rab11 is required for trans-Golgi network-to-plasma membrane transport and a preferential target for GDP dissociation inhibitor.** *Mol Biol Cell* 1998, **9:**3241-3257.

34. Huber LA, Pimplikar S, Parton RG, Virta H, Zerial M, Simons K: **Rab8, a small GTPase involved in vesicular traffic between the TGN and the basolateral plasma membrane.** *J Cell Biol* 1993, **123:**35-45.

35. Peranen J, Auvinen P, Virta H, Wepf R, Simons K: **Rab8 promotes polarized membrane transport through reorganization of actin and microtubules in fibroblasts.** *J Cell Biol* 1996, **135:**153-167.

36. Gawantka V, Ellinger-Ziegelbauer H, Hausen P: **Beta 1-integrin is a maternal protein that is inserted into all newly formed plasma membranes during early *Xenopus* embryogenesis.** *Development* 1992, **115:**595-605.

37. Larkin K, Danilchik MV: **Microtubules are required for completion of cytokinesis in sea urchin eggs.** *Dev Biol* 1999, **214:**215-226.

38. Sulston JE, Schierenberg E, White JG, Thomson JN: **The embryonic cell lineage of the nematode *Caenorhabditis elegans*.** *Dev Biol* 1983, **100:**64-119.

39. Rocheleau CE, Downs WD, Lin R, Wittmann C, Bei Y, Cha YH, *et al.*: **Wnt signaling and an APC-related gene specify endoderm in early *C. elegans* embryos.** *Cell* 1997, **90:**707-716.

40. Thorpe CJ, Schlesinger A, Carter JC, Bowerman B: **Wnt signaling polarizes an early *C. elegans* blastomere to distinguish endoderm from mesoderm.** *Cell* 1997, **90:**695-705.

41. Deng Y, Bennink JR, Kang HC, Haugland RP, Yewdell JW: **Fluorescent conjugates of brefeldin A selectively stain the endoplasmic reticulum and Golgi complex of living cells.** *J Histochem Cytochem* 1995, **43:**907-915.

42. Polishchuk RS, Polishchuk EV, Marra P, Alberti S, Buccione R, Luini A, *et al.*: **Correlative light-electron microscopy reveals the tubular-saccular ultrastructure of carriers operating between Golgi apparatus and plasma membrane.** *J Cell Biol* 2000, **148:**45-58.

43. Ryan TA, Reuter H, Wendland B, Schweizer FE, Tsien RW, Smith SJ: **The kinetics of synaptic vesicle recycling measured at single presynaptic boutons.** *Neuron* 1993, **11:**713-724.

44. Centonze VE, White JG: **Multiphoton excitation provides optical sections from deeper within scattering specimens than confocal imaging.** *Biophys J* 1998, **75:**2015-2024.

45. Mohler WA, White JG: **Stereo-4-D reconstruction and animation from living fluorescent specimens.** *Biotechniques* 1998, **24:**1006-1010, 1012.

46. Bi E, Maddox P, Lew DJ, Salmon ED, McMillan JN, Yeh E, *et al.*: **Involvement of an actomyosin contractile ring in *Saccharomyces cerevisiae* cytokinesis.** *J Cell Biol* 1998, **142:**1301-1312.

47. Togo T, Alderton JM, Bi GQ, Steinhardt RA: **The mechanism of facilitated cell membrane resealing.** *J Cell Sci* 1999, **112:**719-731.

48. Gonczy P, Pichler S, Kirkham M, Hyman AA: **Cytoplasmic dynein is required for distinct aspects of MTOC positioning, including centrosome separation, in the one cell stage *Caenorhabditis elegans* embryo.** *J Cell Biol* 1999, **147:**135-150.

49. Skop AR, White JG: **The dynactin complex is required for cleavage plane specification in early *Caenorhabditis elegans* embryos.** *Curr Biol* 1998, **8:**1110-1116.

50. Shaw SL, Quatrano RS: **The role of targeted secretion in the establishment of cell polarity and the orientation of the division plane in Fucus zygotes.** *Development* 1996, **122:**2623-2630.

51. Schlesinger A, Shelton CA, Maloof JN, Meneghini M, Bowerman B: **Wnt pathway components orient a mitotic spindle in the early *Caenorhabditis elegans* embryo without requiring gene transcription in the responding cell.** *Genes Dev* 1999, **13:**2028-2038.

52. Echard A, Jollivet F, Martinez O, Lacapere JJ, Rousselet A, Janoueix-Lerosey I, *et al.*: **Interaction of a Golgi-associated kinesin-like protein with Rab6.** *Science* 1998, **279:**580-585.

53. Le Bot N, Antony C, White J, Karsenti E, Vernos I: **Role of xklp3, a subunit of the *Xenopus* kinesin II heterotrimeric complex, in membrane transport between the endoplasmic reticulum and the Golgi apparatus.** *J Cell Biol* 1998, **143:**1559-1573.

54. Bi GQ, Morris RL, Liao G, Alderton JM, Scholey JM, Steinhardt RA: **Kinesin- and myosin-driven steps of vesicle recruitment for Ca2+-regulated exocytosis.** *J Cell Biol* 1997, **138:**999-1008.

55. Steinhardt RA, Bi G, Alderton JM: **Cell membrane resealing by a vesicular mechanism similar to neurotransmitter release.** *Science* 1994, **263:**390-393.

56. Hill E, Clarke M, Barr FA: **The Rab6-binding kinesin, Rab6-KIFL, is required for cytokinesis.** *EMBO J* 2000, **19:**5711-5719.

57. Williams BC, Riedy MF, Williams EV, Gatti M, Goldberg ML: **The *Drosophila* kinesin-like protein KLP3A is a midbody component required for central spindle assembly and initiation of cytokinesis.** *J Cell Biol* 1995, **129:**709-723.

58. Jantsch-Plunger V, Gonczy P, Romano A, Schnabel H, Hamill D, Schnabel R, *et al.*: **CYK-4: a Rho family GTPase activating protein (GAP) required for central spindle formation and cytokinesis.** *J Cell Biol* 2000, **149:**1391-1404.

59. Huang JD, Brady ST, Richards BW, Stenolen D, Resau JH, Copeland NG, *et al.*: **Direct interaction of microtubule- and actin-based transport motors.** *Nature* 1999, **397:**267-270.

60. Langford GM: **Actin- and microtubule-dependent organelle motors: interrelationships between the two motility systems.** *Curr Opin Cell Biol* 1995, **7:**82-88.

61. Karpova TS, Reck-Peterson SL, Elkind NB, Mooseker MS, Novick PJ, Cooper JA: **Role of actin and myo2p in polarized secretion and growth of *Saccharomyces cerevisiae*.** *Mol Biol Cell* 2000, **11:**1727-1737.

62. Pruyne D, Bretscher A: **Polarization of cell growth in yeast.** *J Cell Sci* 2000, **113:**571-585.

63. Schott D, Ho J, Pruyne D, Bretscher A: **The COOH-terminal domain of Myo2p, a yeast myosin V, has a direct role in secretory vesicle targeting.** *J Cell Biol* 1999, **147:**791-808.

64. Smith LG: **Divide and conquer: cytokinesis in plant cells.** *Curr Opin Plant Biol* 1999, **2:**447-453.

65. Taunton J, Rowning BA, Coughlin ML, Wu M, Moon RT, Mitchison TJ, *et al.*: **Actin-dependent propulsion of endosomes and lysosomes by recruitment of N-WASP.** *J Cell Biol* 2000, **148:**519-530.

66. Glotzer M: **The mechanism and control of cytokinesis.** *Curr Opin Cell Biol* 1997, **9:**815-823.

67. Waddle JA, Cooper JA, Waterston RH: **Transient localized accumulation of actin in *Caenorhabditis elegans* blastomeres with oriented asymmetric divisions.** *Development* 1994, **120:**2317-2328.

68. Eckley DM, Ainsztein AM, Mackay AM, Goldberg IG, Earnshaw WC: **Chromosomal proteins and cytokinesis: patterns of cleavage furrow formation and inner centromere protein positioning in mitotic heterokaryons and mid-anaphase cells.** *J Cell Biol* 1997, **136:**1169-1183.

69. Kaitna S, Mendoza M, Jantsch-Plunger V, Glotzer M: **Incenp and an aurora-like kinase form a complex essential for chromosome segregation and efficient completion of cytokinesis.** *Curr Biol* 2000, **10:**1172-1181.

70. Adams RR, Tavares AA, Salzberg A, Bellen HJ, Glover DM: ***pavarotti* encodes a kinesin-like protein required to organize the central spindle and contractile ring for cytokinesis.** *Genes Dev* 1998, **12:**1483-1494.

71. Kuriyama R, Dragas-Granoic S, Maekawa T, Vassilev A, Khodjakov A, Kobayashi H: **Heterogeneity and microtubule interaction of the CHO1 antigen, a mitosis-specific kinesin-like protein. Analysis of subdomains expressed in insect sf9 cells.** *J Cell Sci* 1994, **107:**3485-3499.

72. Swan KA, Severson AF, Carter JC, Martin PR, Schnabel H, Schnabel R, *et al.*: **cyk-1: a *C. elegans* FH gene required for a late step in embryonic cytokinesis.** *J Cell Sci* 1998, **111:**2017-2027.

73. Brenner S: **The genetics of *Caenorhabditis elegans*.** *Genetics* 1974, **77:**71-94.

74.   Shelton CA, Bowerman B: **Time-dependent responses to glp-1-mediated inductions in early *C. elegans* embryos.** *Development* 1996, **122:**2043-2050.

75.   Mohler WA, Simske JS, Williams-Masson EM, Hardin JD, White JG: **Dynamics and ultrastructure of developmental cell fusions in the *Caenorhabditis elegans* hypodermis.** *Curr Biol* 1998, **8:**1087-1090.

76.   Mello CC, Kramer JM, Stinchcomb D, Ambros V: **Efficient gene transfer in *C. elegans*: extrachromosomal maintenance and integration of transforming sequences.** *EMBO J* 1991, **10:**3959-3970.

77.   Nonet ML, Staunton JE, Kilgard MP, Fergestad T, Hartwieg E, Horvitz HR, *et al.*: ***Caenorhabditis elegans* rab-3 mutant synapses exhibit impaired function and are partially depleted of vesicles**. *J Neurosci.* 1997, **17:**8061-8073.